# Preparation of cellulose nanocrystals from lignin-rich reject material for oil emulsification in an aqueous environment

**Jonna Ojala[a*], Juho A. Sirviö[a], and Henrikki Liimatainen[a]**

*Jonna Ojala, Researcher, jonna.ojala@oulu.fi (Corresponding author)

Juho Sirviö, Senior Researcher, juho.sirvio@oulu.fi

Henrikki Liimatainen, Associate Professor, henrikki.liimatainen@oulu.fi

[a]University of Oulu, Fibre and Particle Engineering, P.O. Box 4300, FI-90014 Oulu, Finland

## Abstract

Cellulose nanocrystals (CNCs) with amphiphilic features were used in oil drop stabilization in diesel oil-in-water (o/w) emulsion. The functionalized CNCs were synthesized from a lignin-rich reject cellulose source from the pulp and paper industry, i.e., the non-bleached fines fractions of carton pulp. Partial periodate-chlorite oxidation, which was followed by reductive butylamination, was used to obtain surface-modified amphiphilic CNCs. All studied CNCs prevented droplet coalescence by stabilizing oil droplets in the emulsion thus resulting in stable o/w Pickering-like emulsions. CNCs from the fines fractions at concentrations 0.05–0.1% (weight by weight, w/w) provided high stability against creaming (i.e., phase separation), and they did not de-emulsify at low temperatures since the oil droplet size remained small at +5 °C at a 0.05% (w/w) CNC concentration. Salinity improved the stability against creaming with the reference chemical pulp CNC, but negatively affected the emulsion creaming rate for CNCs that had a higher level of lignin. However, the non-bleached fines fraction of the pulp may provide one potential and cost-effective raw material source for the development of a novel bio-based chemical.

**Keywords**

*Nanocellulose, Reject fiber fines, Cellulose nanocrystals, Oil in water emulsion, Bio-based dispersant, Lignin*

## 1. Introduction

Ever increasing oil activities, including oil drilling and oil transportation by sea, increase the risk of oil spills that may be detrimental to the marine ecosystem (Al-Majed et al. 2012). In the larger, nearer to the coast spills, the risk of oil floating into shallow waters is greater, and more severe damage to the environment is likely to occur. The use of surface active oil dispersants is often the most often deployed response option for large spills. Such dispersants enhance the naturally occurring oil slick breaking action caused by wind and waves to obtain sufficiently small droplets to aid microbial degradation (Zeinstra-Helfrich et al. 2015). An effective oil dispersant breaks the oil into small droplets, typically less than 70 microns in diameter, while simultaneously lowering the oil droplet rise velocity and enabling the potential microbial attack before the droplet reaches the ocean's surface (Yu et al. 2014; Prince 2015). Dispersion of oil has reportedly promoted the biodegradation of the oil in the case of deep water spills and also reduced the impact of floating oil on the shoreline (Prince 2015).

Most commercially available chemical dispersants are a mixture of both non-ionic and anionic surfactants, as well as other solvents, which makes the dispersant partially soluble in both oil and water (Al-Majed et al. 2012; Guodong et al. 2015; Nyankson et al. 2015). Synthetic dispersants have been used for decades, even though they appear to have a moderate level of toxicity that adversely affects marine ecosystems (George-Ares and Clark 2000; Zhang et al. 2013; Prince 2015). Therefore, research on new, sustainable, and more

benign dispersants based on natural raw materials is highly desirable. In particular, different bio-based reject materials originating from industrial processes, such as papermaking and biomass processing, are attractive due to their abundance, low cost, and natural biodegradability(Silva et al. 2008; García et al. 2016; Orelma et al. 2017). For example, fiber fines (the small particle size fractions of cellulose pulps), which are typically related to the increased smoothness of paper and board, as well as improved air permeability resistance, are quite problematic in some papermaking processes, such as producing packaging board. The effect of fines on paper and board processing stages, like dewatering and retention, is negative, and when the content of fines increases, the strength properties are getting worse due to poor binding capability of fines. In addition, fiber fines often contain pitch-like materials (stickies), which cause holes and other problems in the manufacture of paper products. Paper and carton manufacturers, especially those working with mechanical pulping, where lignin-rich fines are stiff and do not bond to fibers, find these fines fractions to be less desirable fractions (Gharehkhani et al. 2015). These side-stream fractions are often considered as reject material; therefore, novel applications for the utilization of non-bleached fiber fines are desirable.

Nanomaterials are typically considered to be materials which are in the form of particles, tubes, fibers or rods and have at least one dimension between 1 to 100 nm. Technologies that include different nanosized materials, such as nanowires, magnetic composites/gels, or bio-based nanoparticles, may provide alternative methods to control oil spills in the marine environment(Saha et al. 2013; Wang et al. 2013; Pi et al. 2016; Daza et al. 2017) These applications are based on tuned hydrophobicity through creating complexes or

surface coatings that enable oil adsorption. Bio-based nanoparticles, such as cellulose nanocrystals and -fibrils, have been under research for finding new environmentally friendly dispersants for enhanced oil spill recovery. However, naturally hydrophilic cellulose typically requires chemical modifications, including the attachment of hydrophobic functional groups, to improve its ability to stabilize o/w emulsions (Xhanari et al. 2011). Naturally, more hydrophobic raw materials such as lignin-rich fiber fines provide a raw material that is cheaper and is assumed to function better on hydrophobic matrices.

The ability of different kinds of nanoparticles to adsorb at interfaces is a known phenomenon that has been utilized broadly in the emulsion stabilization in so-called Pickering emulsions (Kalashnikova et al. 2011, 2013; Chevalier and Bolzinger 2013; Jiang et al. 2014; Hu et al. 2015a, 2015b). Within nanoparticle stabilized emulsions, the creaming phenomenon has been reported as the most probable route for de-stabilization. Creaming refers to the separation of phases while the oil droplet size remains stable in the floating creamy oil phase without oil droplet coalescence. Amphiphilic bifunctionalized cellulose nanoparticles are able to form Pickering-like emulsions, stabilizing the oil droplet against coalescence by adsorbing into the oil water interface covering the oil droplet (Ojala et al. 2016). Moreover, those functionalized nanoparticles are predicted to slow down the creaming phenomenon, thus, potentially make the natural biodegradation of oil more efficient.

In this work, amphiphilic cellulose nanocrystals (CNC) were used as dispersing and stabilizing agents in diesel o/w emulsions in an aqueous environment. The cellulose nanocrystals were synthesized from lignin-rich fiber fines, a side product of carton

production, through partial periodate-chlorite oxidation and reductive amination, followed by a homogenization phase to liberate individual bifunctionalized cellulose nanocrystals (Sirvio et al. 2011). Unbleached fines fractions have high lignin content believed to promote their inherent hydrophobicity and feasibility for oil dispersion and stabilization material fabrication. Altogether, three different samples were fabricated. Two cellulose nanocrystal samples were made from the lignin-rich, semi-chemical pulp fines fractions CNC-Lig-1 and CNC-Lig-2. One sample was made from a low-lignin birch pulp (Kraft pulp) (CNC-CHEM). The CNC suspensions were characterized with a transmission electron microscope (TEM), while the dispersion effectiveness was addressed by measuring the oil droplet size in emulsion along with the emulsion stability. The oil droplet size and o/w emulsion stability measurements were conducted at a room temperature of 20°C and at 5°C to simulate the colder water environment.

## 2. Materials and Methods

### *2.1. Materials*

Semi-chemical hardwood pulp from corrugated board manufacturing was obtained from a Finnish mill as a readily refined pulp suspension from which a fines fraction was separated for nanocellulose synthesis. Kraft pulp, i.e., chemical birch pulp (*Betula Pendula*), was received as dry sheets and was then disintegrated into water according to standard procedure (ISO 5263-1:2004). The chemical composition of the cellulose materials that were

used was determined according to standard procedures for wood extractives (SCAN-CM 49:03 standard), hemicelluloses (TAPPI-T Method 212 om-02), and lignin (TAPPI-T Method 222 om-02).

All of the chemicals used in the periodate and chlorite oxidations ($NaIO_4$, $NaClO_2$, and $CH_3COOH$) and aldehyde and carboxyl content analyses ($NH_2OH{\cdot}HCl$, $CH_3COONa{\cdot}2H_2O$, NaCl, and NaOH) were pro analysis (p.a.) grade obtained from Sigma−Aldrich (Germany). In the reductive amination reaction, 2-picoline borane (Sigma-Aldrich, St. Louis, MO, USA [95%]) and *n*-butylamine hydrochloride (Tokyo Chemical Industry, Belgium [> 98%]) were used. Ethanol ($C_2H_6O$; purity ~96%), obtained from VWR International GmbH (Finland), and hydrochloric acid (HCl) from Sigma-Aldrich (Germany) were used in the washing steps after the amination process. All chemicals were p.a. grade and were used without further purification. Deionized water was used in all dilutions and washing steps throughout the experiments. Lightweight, sulphur-free, winter grade marine diesel oil (Neste Oil, Finland) with a density of 828 kg/m$^3$ at 15 °C and a viscosity of 1.846 mm$^2$s$^{-1}$ at 40 °C was used for all o/w emulsions.

### *2.2. Preparation of synthetic seawater*

To mimic oceanic conditions, synthetic seawater was prepared according to the modified formula of Kester et al. (1967). The composition of synthetic seawater is presented in Table 1. Briefly, the gravimetric salts were used in anhydrous form after drying them overnight in an oven. Reagents containing the water of hydration were first weighed, then diluted to be

used as a stock solution. The pH of the readily made seawater was 8.5, conductivity was 19.3 [mS/cm], and salinity was 3.5%. The freshly prepared seawater was sterilized 121 °C at 1 bar for 15 min to prevent any microbial growth.

| **Gravimetric salts** | **Amount [g/kg of the solution]** | **Concentration [mmol/L]** |
|---|---|---|
| NaCl | 23.926 | 409.41 |
| $Na_2SO_4$ | 4.008 | 28.22 |
| KCl | 0.677 | 9.08 |
| $NaHCO_3$ | 0.196 | 2.33 |
| KBr | 0.098 | 0.82 |
| $H_3BO_3$ | 0.026 | 0.42 |
| NaF | 0.003 | 0.07 |
| **Volumetric salts** | **Concentration [mmol/ L]** | |
| $MgCl_2{\cdot}6H_2O$ | 53.7 | |
| $CaCl_2{\cdot}2H_2O$ | 10.33 | |
| $SrCl_2{\cdot}6H_2O$ | 0.09 | |

Table 1. Composition of synthetic seawater.

*2.3. Fabrication of butylamino-functionalized CNCs*

*2.3.1 Separation of a fines fraction from semi-chemical pulp*

A fraction containing only the fines material (particles < 150 µm) was separated from the semi-chemical pulp by screening with a 100 mesh screen under constant water flow. The suspension was then concentrated through a 20 µm filtering cloth to obtain a sample with a dry matter content of approximately 10%. This material was used to fabricate functionalized CNCs.

*2.3.2. The chemical oxidation-amination pre-treatment*

The bifunctionalized CNCs with amphiphilic nature were prepared using a combination of oxidative chemical pre-treatments, followed by amination with butylamine and finally a mechanical homogenization phase, to liberate the individual nanocrystals.

The fabrication was initiated by oxidizing the fines fraction of the semi-chemical pulp with metaperiodate to result in two diverse aldehyde contents (DAC_A and DAC_B). In the procedure, wet cellulose pulp (15 g oven-dry weight) was oxidized using 12.3 g of sodium periodate ($NaIO_4$) in deionized water (1,500 ml) at 65 °C for 180 min to attain DAC_A. DAC_B was prepared similarly, except that 27 g of lithium chloride (LiCl) was used as an additive and the temperature setting was 75 °C. The third product, DAC_C, was prepared using similar chemistry as that used for the DAC_B, but Kraft pulp was used as a raw material.

In the second step, sodium chlorite ($NaClO_2$) was used to partially oxidize the aldehydes of the DACs to obtain dicarboxylic acid groups (PO-DACs). The amounts of sodium chlorite used were 0.497 g, 0.80 g, and 0.80 g for DAC_A, DAC_B, and DAC_C, respectively. Sodium chlorite was first diluted with 17.78 g of deionized water, and then poured into a beaker with 26.65 ml of 20 vol% acetic acid. These solutions were then mixed with 2 g of DAC, oxidized, and then diluted in 44.4 ml of water. The oxidation reaction was completed under a fume hood with continuous mixing for 8 min. The three cellulose products obtained were labeled PO-DAC/A, PO-DAC/B, and PO-DAC/C.

Reductive amination was then used to introduce *n*-butylamino groups to the oxidized cellulose. The amination for DAC_A was conducted by adding 7.37 g *n*-butylamine

hydrochloride to 200 ml of deionized water and adjusting the pH to 4.5 with a diluted HCl solution. For DAC_B and DAC_C, 12.19 g of *n*-butylamine were used. Next, a 2-picoline borane solution, where 1.44 g (for DAC_A) and 2.38 g (for both DAC_B and DAC_C) had been diluted in 200 ml deionized water, was added to the *n*-butylamine hydrochloride solution, and 4 g of each PO-DAC fiber sample were also weighed. After 72 h of continuous mixing at room temperature, the samples were filtered to stop the reaction and were washed with water (V = 200 ml) and ethanol (V = 300 ml). Finally, the solid was collected into a beaker, and a 200 ml 0.1 M HCl solution was added. After 5 min of mixing, the suspension was filtered and washed with 500 ml of deionized water. This procedure resulted in three different bifunctionalized samples.

*2.3.3. Liberation of nanoparticles from chemically pre-treated celluloses*

The bifunctionalized cellulose materials were converted to individual CNCs with a solids content of 0.1 wt% and a pH of 10 (pH was adjusted using NaOH) using a homogenization treatment with an M-110EH−30 microfluidizer (Microfluidics, Newton, MA, USA). The suspensions were passed once through a combination of a 400 µm auxiliary processing module (APM) and 200 µm interaction chamber (IXC) at a pressure of 1,300 bar followed by passage through a combination of 400 µm APM and 100 µm IXC at a pressure of 1,700 bar.

Finally, the cellulose nanoparticles were labelled as CNC-LIG-1, CNC-LIG-2, and CNC-CHEM to indicate the bifunctionalized nanocrystals (CNC-LIG-1 and CNC-LIG-2 from the lignin-rich semi-chemical pulp and CNC-CHEM from the Kraft pulp).

196

197 *2.4. Determination of initial aldehyde content and carboxyl content after oxidation pre-*
198 *treatment*

199 The initial aldehyde content of celluloses after sodium periodate oxidation was analyzed
200 through an oxime reaction, which is described in more detail elsewhere (Sirvio et al. 2011).
201 Briefly, the reaction is based on the premise that one mole of aldehyde in oxidized cellulose
202 reacts with one mole of $NH_2OH$•HCl, and, after the reaction, the nitrogen content can be
203 determined from a freeze-dried sample by using an elemental analyzer (PerkinElmer
204 CHNS/O 2400 Series II; PerkinElmer, Waltham, MA, USA). The aldehyde content can then
205 be calculated straight from the known nitrogen content. The carboxyl content of the
206 dicarboxylic acid samples was determined with conductometric titration as described by
207 Katz et al. (1984) and Rattaz et al. (2011).

208

209 *2.5. Determination of the amino groups of bifunctionalized celluloses*

210 The samples were freeze-dried (Scanvac CoolSafe; Labogene Aps, Lygne, Denmark) at a
211 solids content of 0.1 wt% for 60 h prior to elemental analysis. The CHN/O 2400 organic
212 elemental analyzer (PerkinElmer, Waltham, MA, USA) was used to determine the nitrogen
213 content of the samples from which the number of amino groups was calculated.

214

215 *2.6. Transmission electron microscopy (TEM)*

The morphological features of the fabricated nanocelluloses were analyzed with a Tecnai G2 Spirit TEM (FEI Europe, Eindhoven, the Netherlands). Samples were prepared by diluting each sample with ultrapure water. A small droplet of the dilution was added on top of a Butvar-coated copper grid. The excess amount of the sample was removed from the grid by touching the droplet with the corner of a filter paper. Negative staining of the samples was performed by placing a droplet of uranyl acetate (2% w/v) on top of each specimen. The excess uranyl acetate was removed with filter paper as described above. The grids were dried at room temperature and analyzed at 100 kV under standard conditions. Images were captured using a Quemesa CCD camera and iTEM image analysis software (Olympus Soft Imaging Solutions GMBH, Munster, Germany) to measure the width of the individual nanocelluloses. In total, at least 50 crystals of each sample were measured. The final results were averaged and standard deviations were calculated.

*2.7. Formation of diesel o/w emulsion and droplet stabilization using cellulose nanocrystals*

To determine the influence of the CNCs (CNC-LIG-1–2 and CNC-CHEM) on o/w emulsification, the nanocelluloses were mixed with the water phase before oil was added and dispersed. The final nanocellulose concentrations varied from 0.05% to 0.1% (w/w). The emulsions were prepared using the UltraTurrax mixer (IKA T25; IKA-Works, Staufen im Breisgau, Germany) at 7,000 rpm for 15 min and maintaining the 1:10 oil to water ratio throughout the study. To monitor the stability in cold conditions, some emulsions were

prepared using cooled (approx. 5 ± 2 °C) water, and the samples were held in an ice bath to prevent warming during dispersing.

### *2.8. Particle size analysis and microscopy*

The changes in oil droplet size were analyzed using a laser diffraction particle size analyzer (LS 13 320; Beckman Coulter, Indianapolis, IN, USA). Each sample was measured directly after dispersing, and three parallel measurements were performed. Droplet sizes of samples were observed and imaged using a LeicaMZ LIII stereomicroscope (Leica Microsystems Ltd., Heerbrugg, Switzerland) to visualize oil droplet density, size, and possible aggregation after dispersion.

### *2.9. Emulsion stability analysis with analytical centrifuge*

An analytical centrifuge (LUMiFuge; LUM GmbH, Berlin, Germany) was used to evaluate the o/w emulsion stability at room temperature and at a cold temperature (5 °C) mimicking the conditions prevailing in cold seawaters. The centrifuge detects the emulsion stability and demixing phenomena during centrifugation by measuring the changes in light transmittance at an 800 nm wavelength over the whole sample height. A 1,200 rpm rotational speed, corresponding to a relative centrifugal force of 205 G, was used. Changes in transmission indicate phase separation through creaming. A measurement at 30 min reveals the creaming process as a function of time, whereas lower transmission values

indicate better stability against creaming. At least two parallel measurements of each sample were analyzed.

### *2.10. Interfacial tension by surface tensiometer*

The du Noüy ring method was used to measure the changes in the surface tension of aqueous suspensions of functionalized nanoparticles as a function of concentration at room temperature (du Noüy 1925). Distilled water and pure diesel oil were also measured as references.

In the du Noüy method, a platinum wire ring lying in a plane parallel to the undisturbed liquid surface is submerged in the liquid and then slowly withdrawn, while the net fluid force on the ring is measured. The force ($F$) that is required to raise the ring from the liquid is measured and related to the liquid's surface tension ($\gamma$). The maximum force ($F_{max}$) that is obtained by the ring can be directly related to the interfacial tension using Equation 1:

$$\boldsymbol{F = 2\pi \cdot (r_i + r_o) \cdot \gamma}, \qquad \textbf{(1)}$$

where $r_i$ is the radius of the inner ring of the liquid film pulled, and $r_o$ is the radius of the outer ring of the liquid film.

## 3. Results and discussion

### *3.1. Characteristics of cellulose fines raw material*

Amphiphilic cellulose nanocrystals were produced from the fines fraction of the semi-chemical pulp and Kraft pulp fibers (reference sample) by using combined oxidation and reductive amination treatments. The semi-chemically produced corrugated board pulp was first fractionated with a 150 µm slot hole sieve to obtain a fraction containing only the fines particles, and then analyzed to determine their average length and width, as well as size distribution. The average (length-weighted) length and width of the hardwood pulp fibers, determined using a Metso FiberLab image analyzer (Metso Automation, Helsinki, Finland), were 0.65 mm and 21.2 µm, respectively. After screening the original sample, a different fraction was obtained. The average length in the fines fraction was roughly half that of the original pulp fibers, 0.30 mm, while the average width was 16.2 µm. The fines fraction consists of mainly split or cut fibers, or external fibrils, originating from the pulp refining stage (Koskenhely 2008). The wood extractives, hemicellulose, and lignin contents of the original semi-chemical pulp were 1.8%, 14.1%, and 14.7%, respectively, and, for the Kraft pulp (reference sample), they were 0.08%, 24.7%, and 0.4%, respectively. Thus, the cellulose content was 70.4% for the semi-chemical pulp and 74.8% for the Kraft pulp. The wood extractives' content of the separated fines fraction was 0.1%, content of hemicelluloses was 4.8%, and total lignin content was 37.3%.

The chemical analysis revealed a high content of lignin in the fines fraction. The lignin content of the original pulp was 14.7%, but, in the fines fraction, the lignin content was 37.3%. A possible explanation of this phenomenon is that lignin is located in the outer layer of the fibers and removed easily when fines are peeled from the fiber surface during the pulp refining treatment. Due to the high lignin content, the fines fraction was expected to

297 be naturally more hydrophobic than the Kraft pulp fibers, which increases its stabilization
298 potential in oil emulsification applications. Typically, chemical pulp contains less than 15%
299 fines content (Ek et al. 2009) which causes problems in paper manufacture due to their
300 poor quality and binding ability. Therefore, they are normally rejected from the process.

301

302 *3.2. Chemical properties of bifunctionalized CNCs*

303 CNCs were liberated from the fines fraction of the semi-chemical pulp and Kraft pulp fibers
304 after combined oxidation and reductive amination treatments, followed by mechanical
305 homogenization. These chemical reaction routes were described in a previous publication
306 (Ojala et al. 2016). The aldehyde and carboxyl contents of the cellulose, after periodate and
307 chlorite oxidation, and the butylamino group contents of the nanocelluloses (CNC-LIG-1–2
308 and CNC-CHEM) are shown in Table 2. The initial aldehyde contents were similar for CNC-
309 LIG-1 and CNC-LIG-2 at 2.43 mmol $g^{-1}$ and 2.62 mmol $g^{-1}$, respectively, despite different
310 oxidation temperatures and chemical doses. It is possible that the high lignin content affects
311 negatively to the oxidation by consuming the oxidant for reactions of lignin (Gosselink et al.
312 2011). This assumption is supported by the fact that the CNC-CHEM (made from low-lignin
313 Kraft pulp) had a 32% higher aldehyde content (3.86 mmol $g^{-1}$) than CNC-LIG-2, despite a
314 similar oxidation treatment. On the other hand, the high aldehyde content of CNC-LIG-1
315 may indicate the presence of metals or other impurities that catalyze the reaction, and,
316 thus, result in a higher aldehyde content. The analyzed carboxyl contents revealed that the
317 conversion rates in the carboxylation reaction were 28.8%, 61.1%, and 25.9% for CNC-LIG-

318 1, CNC-LIG-2, and CNC-CHEM, respectively, while the *n*-butylamine contents of aminated
319 nanocelluloses were 0.85 mmol $g^{-1}$, 0.49 mmol $g^{-1}$, and 0.86 mmol $g^{-1}$, respectively. These
320 values correspond to the conversion rates of 35.0%, 18.7%, and 22.3%, respectively. The
321 residual aldehydes were converted into alcohol groups by the reductive agent used in the
322 amination reaction step.
323
324 Table 2. Aldehyde and the carboxyl contents of bifunctionalized CNC samples with *n*-
325 butylamine groups attached.
326

| Sample | Initial aldehydes (mmol $g^{-1}$) | Carboxylic acid content (mmol $g^{-1}$ ) | Amino group content ( mmol $g^{-1}$) |
|---|---|---|---|
| CNC-LIG-1 | 2.43 | 0.7 | 0.85 |
| CNC-LIG-2 | 2.62 | 1.6 | 0.49 |
| CNC-CHEM | 3.86 | 1.0 | 0.86 |

327 *3.3. Morphology of modified nanocelluloses*
328 The morphology of the functionalized cellulose nanocrystals was visualized with TEM, and
329 image analysis was used to average the lengths and the widths of the individual CNCs from
330 the samples. The TEM images of isolated nanocrystals from semi-chemical pulp cellulose
331 are shown in Fig. 1. CNC-LIG-1 revealed rod-like, single crystalline CNCs, with lengths of 40
332 to 100 nm and lateral dimensions from 2 to 4 nm (Fig. 1). The images also revealed the
333 presence of nanofibrils in the samples, since all of the fibers did not disintegrate into
334 crystals, and the suspension was studied unpurified. The size distribution for the CNC-LIG-2
335 was wide, and some of the cellulose nanocrystals and nanofibers were agglomerated; still,
336 most of the material was liberated into crystalline form. The lengths varied from

approximately 60 to 400 nm, though it was not always obvious if it was one fibril or several crystals aligned. However, the average length of the CNC-LIG-2 was 160 nm, and the lateral dimensions varied from 2 to 4 nm. The CNC-CHEM made from Kraft cellulose was thoroughly liberated into individual crystals with similar size distributions, as reported earlier by Ojala et al. (2016), so the average length of one cellulose nanocrystal was approximately 60 to 70 nm, and the lateral dimension was 3 nm.

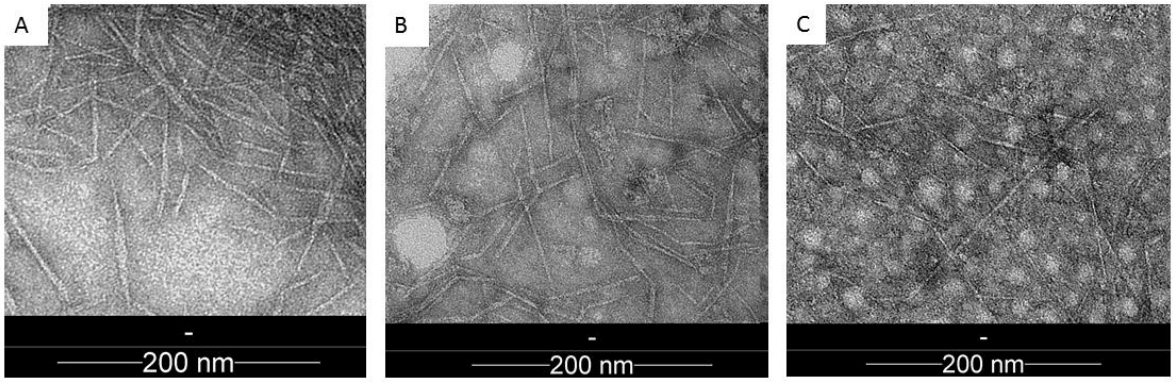


Figure 1. TEM images of a bifunctionalized CNC-CHEM (A) originated from Kraft pulp and CNC-LIG-1 and CNC-LIG-2 (B and C) made from a fines fraction of semi-chemical pulp.

*3.4. Emulsion creaming stability and droplet size measurements*

Diesel o/w emulsions were formed using cellulose nanocrystals as stabilizers. The o/w ratio remained at a constant 10% (w/w) oil level during all experiments. The oil droplet sizes and their distribution from the emulsion were analyzed with the laser diffraction particle size analyzer. The distributions of oil droplet sizes are presented as volume versus size in Figure

353 2. At a nanocellulose concentration of 0.05%, the droplet sizes were in the range of 8.7–
354 13.6 µm when measured at room temperature, while the reference emulsion, without any
355 added nanocellulose, had a droplet size of about 50 µm and was unstable. The measured
356 average droplet sizes and standard deviations are shown in Table 3. The CNC-LIG-2 in a
357 0.05% concentration resulted in the smallest oil droplet size and performed well in cold
358 conditions. A decrease in the dispersing temperature had an obvious effect on the particle
359 sizes of CNC-CHEM; the average particle size increased from 13.6 to 22.2 µm. However, the
360 higher nanocellulose concentration of 0.1% compensated for the particle size increase
361 caused by the lower temperature, and the droplet sizes were the same as those of the
362 0.05% concentration at room temperature. CNC-LIG-1 and CNC-LIG-2 did not show any
363 change in the stabilized oil droplet size at the lower temperature according to mean droplet
364 size. However, the distribution of the oil droplet sizes in the Figure 2 shows the higher
365 amount of smaller droplets when CNC-LIG-1 and CNC-LIG-2 are used.

| CNC used in emulsion | Concentration (%) | Temperature (°C) | Mean (µm) | Standard deviation (µm) |
|---|---|---|---|---|
| **CNC-LIG-1** | 0.05 | +20 | 11.0 | 7.7 |
| | 0.05 | +5 | 13.1 | 9.2 |
| | 0.10 | +5 | 8.3 | 6.4 |
| **CNC-LIG-2** | 0.05 | +20 | 8.7 | 6.0 |
| | 0.05 | +5 | 7.2 | 5.7 |
| | 0.10 | +5 | 7.2 | 5.6 |
| **CNC-CHEM** | 0.05 | +20 | 13.6 | 7.1 |
| | 0.05 | +5 | 22.2 | 13.3 |
| | 0.10 | +5 | 12.4 | 8.7 |

366

Table 3. Average oil droplet sizes of o/w emulsions in different CNC -concentrations and temperatures.

Visual analysis of the sizes of the oil droplets was done through stereomicroscopy from the readily made o/w emulsions. A small aliquot of the emulsion was placed on a glass slide and covered with a glass coverslip. The images (Fig.3) of the oil droplets were observed, and size results were comparable to those obtained from the particle size analysis.

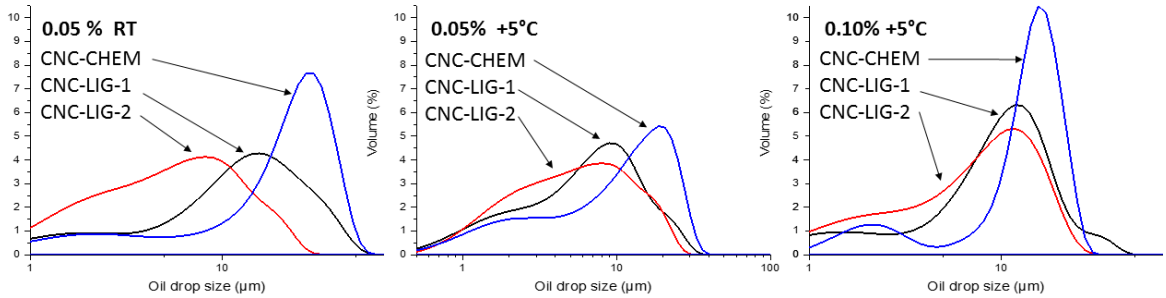


Figure 2. Droplet diameter distributions of emulsions stabilized by CNC-LIG-1, CNC-LIG-2 and CNC-CHEM in concentrations of 0.05% and 0.10 % (on the left). Distributions were analyzed at both room temperature and at +5 °C.

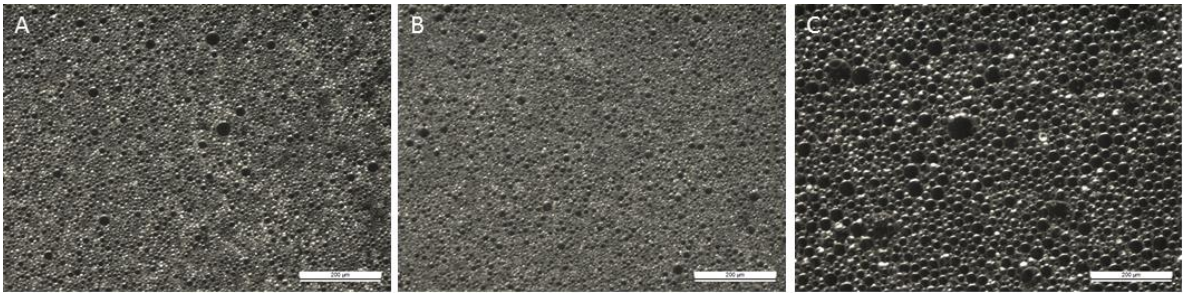


Figure 3. Stereomicroscopy images of CNC-stabilized o/w emulsion at 0.05% (w/w) CNC-LIG-1 (A), CNC-LIG-2 (B) and CNC-CHEM (C) using 10% (w/w) of oil content.

O/w emulsion creaming stability was determined with the LUMifuge analytical centrifuge by monitoring the formation of the creaming layer. The stability analysis was done on a 0.05% (w/w) nanoparticle concentration at room temperature and in two different CNC concentrations, 0.05% and 0.1% (w/w), at a colder +5 °C temperature. Figure 4 illustrates the stability behavior against creaming of emulsions as a function of time. The stability at room temperature with a 0.05% (w/w) CNC concentration was clearly improved since the CNC-LIG-1 reached the final 43% transmission rate and the CNC-LIG-2 slowly increased only at 30% transmittance during the analysis time. The creaming occurred with CNC-CHEM soon after the analysis started (at a concentration of 0.05%), the transmission was approximately 50% after 10 min of centrifugation, and this sample finally reached a 70% transmission rate.

The CNCs obtained from the fines fraction of the semi-chemical pulp seemed to work better compared to the Kraft cellulose nanocrystals, probably due to more naturally hydrophobic surface characteristics. For those CNCs, the creaming was slower (CNC-LIG-1 and CNC-LIG-2), and no droplet coalescence occurred.

Usually, creaming increases the risk of oil droplet coalescence; this means that the forces, which keep the surface between the oil droplets thick enough, weaken and the oil droplets fuse together forming larger droplets (Tadros 2013). In this work, the stability of all studied samples improved in the colder conditions. The lower temperature decreased the thermal motion of droplets and increased the viscosity of fluids, and it therefore reduced the rate of phase separation. The creaming occurred, but the separation was very slow, especially

with CNC-LIG-2. The final transmission rate for CNC-LIG-2, during analysis time, was 5%. CNC-LIG-1 did not perform as well at a concentration of 0.05% (w/w), but increasing the concentration of CNCs to 0.1% (w/w) resulted in improved stability and approximately 10% final transmission. The CNC-CHEM had the most significant differences between different temperatures and concentrations of CNCs, but it still performed as well as the CNC-LIG-1 and CNC-LIG-2 when the dispersant concentration was 0.1%.

In the figure 4, the differences in emulsion stability between different CNC –samples in same physical conditions are clearly shown. It can be detected that in lower concentration (0.05% CNC), CNC-LIG-1 and CNC-LIG-2 performed better than CNC-CHEM, as the transmission level was lower ie. the creaming occurred more slowly. In 0.10% (w/w) CNC concentration there were no differences in transmittance.

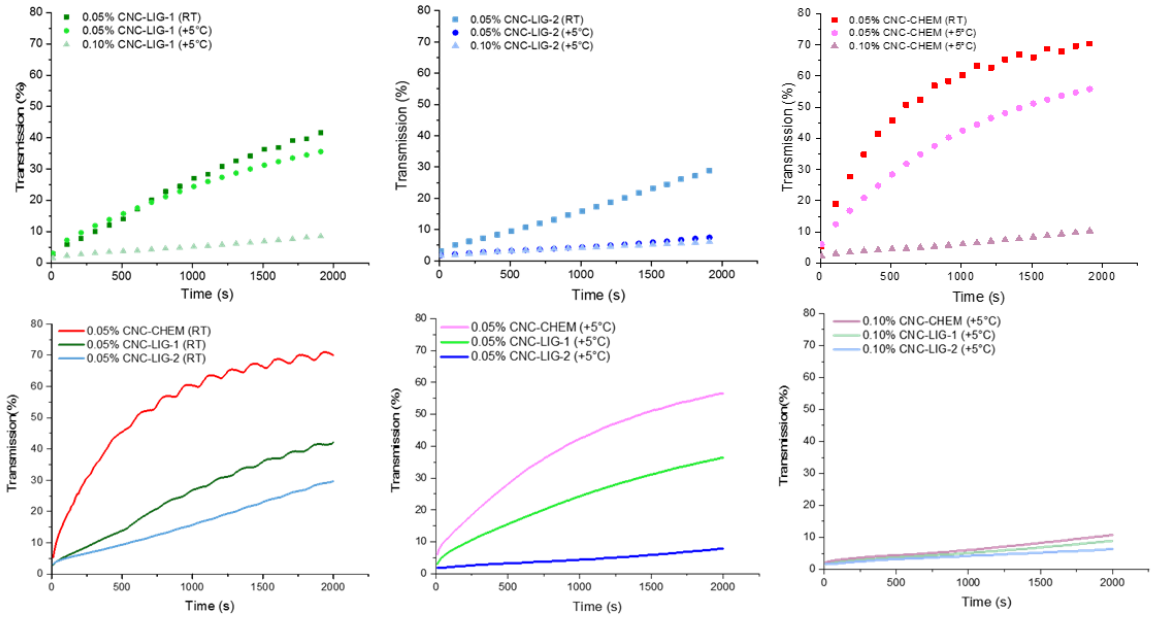


413

Figure 4. Transmission against time for o/w emulsions stabilized with butylamino-functionalized nanocellulose dispersants during centrifugation at 1,200 rpm rotational speed for 30 minutes. CNC-LIG-1 (up-left), CNC-LIG-2 (up-middle), and CNC-CHEM (up-right) were studied in 0.05% (w/w) and 0.10% (w/w) concentrations at both room temperature (+20 °C) and +5 °C.

*3.5. Surface tension reduction using dispersants*

A variety of dispersants are used in applications where interfacial tension between two phases is too high to form stable emulsions. Hydrophobized cellulose CNC suspension can act as a dispersant and change a liquid's wetting characteristics by altering the surface tension at liquid interfaces. In this work, the surface tensions, in different concentrations for the series of samples with butylamino-functionalized CNCs in water, were determined with the du Noüy ring method.

Figure 5 shows the decreasing surface tension $\gamma_{AW}$ of both bifunctionalized CNCs when added to the water already at low concentrations. The initial value for pure water was 72.4 mN/m at room temperature. The dispersant concentrations varied from 0.01–0.1% w/v, and, compared to plain water, the surface tension decreased 11% when CNC-LIG-1 was mixed with water at a 0.1% (w/v) concentration and 26% when the CNC-LIG-2 concentration was at 0.1% (w/v) in water. This reduction of interfacial tension improves the dispersion of oil, and smaller oil droplet sizes in the emulsion are formed.

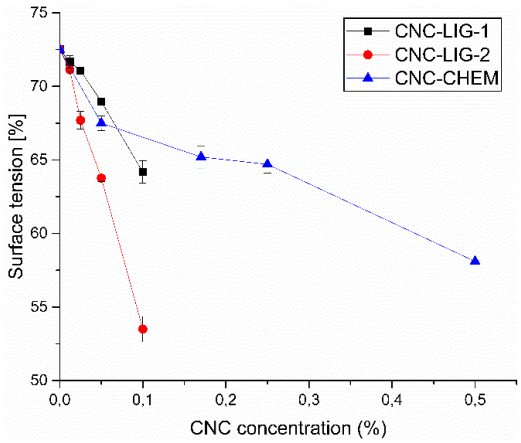


434

435 Figure 5. Air/deionized water surface tension at different CNC concentrations. In
436 comparison, pure deionized water $\gamma_{AW}$ was 72.4 mN/m at 24 °C, while surface tension with
437 0.10% (w/w) CNC-LIG-1 was 64.2 mN/m and with 0.10% (w/w) CNC-LIG-2 53.5 mN/m.

438

439 *3.6. Reject cellulose nanomaterial as an emulsion stabilizer in cold seawater*

440 To study the effect on the marine environment of the cellulose-based biochemicals and
441 their effectiveness on o/w emulsion stability, synthetic seawater was prepared, and oil
442 droplet size and emulsion stability were measured from emulsions stabilized with all CNC

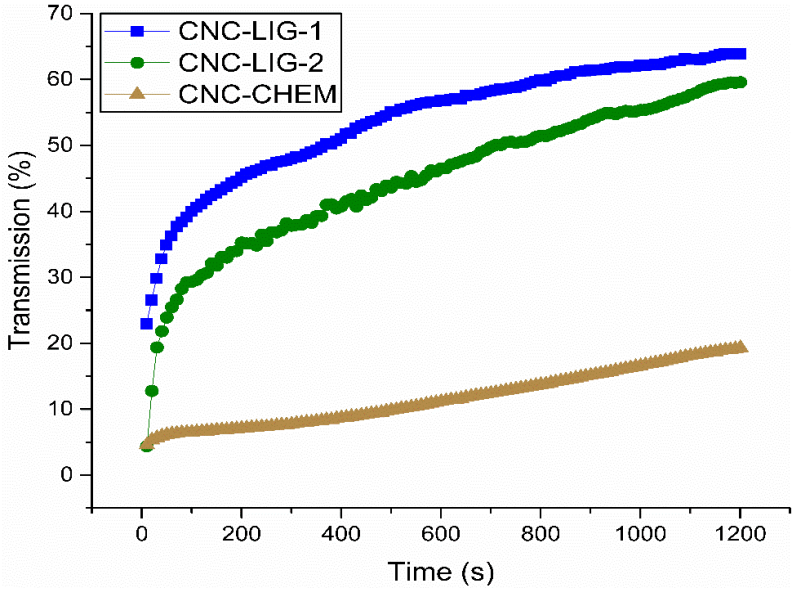

443 samples at a concentration of 0.05%. Immediately after emulsification, all samples seemed
444 to be uniform, and emulsion formation was good. However, the creaming effect was
445 detected very soon after emulsification, which was in agreement with the stability analysis
446 performed with the LUMifuge. No visual droplet coalescence was observed in any of the
447 studied samples. In this experiment, the results showed that the CNC-CHEM performed best
448 in saline conditions. The phase separation was slow, and the emulsion stability remained
449 good. The final transmission rate for CNC-CHEM was approximately 20%. These results are
450 presented in Figure 6.

451 Figure 6. Emulsion stability in cold, synthetic (+5 °C) seawater at a low concentration of
452 CNCs at 0.05% w/w.

453 The results revealed that the effect of low temperature was not as significant as the saline
454 environment on the oil droplet size or on the emulsion stability. The CNC-LIG-2 made from
455 the fines fraction performed well in the 0.05% concentration when standard cold water was
456 used, but the 3.5% salinity negatively affected the stability of the emulsion. On the other
457 hand, CNC-CHEM performed better in the synthetic seawater when already at a low
458 concentration (0.05%). It is probably due to weaker interactions with oil and lignin-rich CNCs
459 in this pH and high salinity. Since no coalescence of oil was visually observed, it is assumed,
460 that the steric barrier is good enough to prevent oil drops separated and the background
461 salt effects only on creaming that is not a negative phenomenon when application in
462 enhanced oil recovery is considered.

463 **Conclusions**

In this work, unpurified, lignin-rich reject cellulose fiber fines were used to produce a novel nanoparticle dispersant containing modified CNCs. A chemical modification route was used to fabricate bifunctionalized nanocelluloses to improve diesel oil dispersing and simultaneous oil droplet stabilization in an o/w emulsion. This study indicated that there is the potential to also utilize reject cellulose material, i.e., fiber fines, in the fabrication of bio-based dispersing and stabilizing agents for o/w emulsion stabilization. Having demonstrated the utilization of cellulose-based nanoparticles as a raw material in the fabrication of a bio-based dispersant, our study indicates that future studies should further investigate the interactions between cellulose nanoparticles and dispersed oil droplets. Moreover, the stabilization mechanisms in deionized water and in saline environments are interesting, since the low temperature was not as significant as the saline environment in affecting the oil droplet size or the stability characteristics of the emulsion in standard water. The high lignin content in pulp promotes the natural hydrophobicity, and, therefore, the wood possesses properties that suggest the potential for other applications such as the oil spill response. Although some interactions between oil droplets and amphiphilic nanoparticles can be explained by steric stabilization, the effect of electrostatic repulsions on emulsion stability still requires more detailed study.

**Acknowledgements**

484 This study was funded by the Academy of Finland (283187). The support of the Ahti Pekkala
485 Foundation and the Tiina and Antti Herlin Foundation is gratefully acknowledged. The
486 contribution of Mr. Mikael Karjalainen in the raw material characterization and the
487 experience of Dr. Ilkka Miinalainen in TEM measurements are also much appreciated. We
488 thank Neste Oyj Finland for providing the marine diesel oil sample for the experiments.

489

490 **References**

491 Al-Majed AA, Adebayo AR, Hossain ME (2012) A sustainable approach to controlling oil spills. J
492 Environ Manage 113:213–227. doi: 10.1016/j.jenvman.2012.07.034

493 Chevalier Y, Bolzinger M-A (2013) Emulsions stabilized with solid nanoparticles: Pickering
494 emulsions. Colloids Surf Physicochem Eng Asp 439:23–34. doi:
495 10.1016/j.colsurfa.2013.02.054

496 Daza EA, Misra SK, Scott J, et al (2017) Multi-Shell Nano-CarboScavengers for Petroleum Spill
497 Remediation. Sci Rep 7:41880. doi: 10.1038/srep41880

498 Du Nouy PL (1925) AN INTERFACIAL TENSIOMETER FOR UNIVERSAL USE. J Gen Physiol 7:625–631.
499 doi: 10.1085/jgp.7.5.625

500 Ek M, Gellerstedt G, Henriksson G (2009) Pulping Chemistry and Technology. In: Pulp and Paper
501 Chemistry and Technology. De Gruyter, Berlin,

502 García A, Gandini A, Labidi J, et al (2016) Industrial and crop wastes: A new source for
503 nanocellulose biorefinery. Ind Crops Prod 93:26–38. doi: 10.1016/j.indcrop.2016.06.004

504 George-Ares A, Clark JR (2000) Aquatic toxicity of two Corexit® dispersants. Chemosphere 40:897–
505 906. doi: 10.1016/S0045-6535(99)00498-1

506 Gharehkhani S, Sadeghinezhad E, Kazi SN, et al (2015) Basic effects of pulp refining on fiber
507 properties—A review. Carbohydr Polym 115:785–803. doi: 10.1016/j.carbpol.2014.08.047

508 Gosselink RJA, van Dam JEG, de Jong E, et al (2011) Effect of periodate on lignin for wood adhesive
509 application. Holzforschung. doi: 10.1515/hf.2011.025

510 Guodong Q, Yupeng Z, Xuhe R, Jie C (2015) Research on Development and Effectiveness Evaluation
511 Technology of New Environment-friendly Oil Spill Dispersant. Aquat Procedia 3:245–253.
512 doi: 10.1016/j.aqpro.2015.02.218

513 Hu Z, Ballinger S, Pelton R, Cranston ED (2015a) Surfactant-enhanced cellulose nanocrystal
514 Pickering emulsions. J Colloid Interface Sci 439:139–148. doi: 10.1016/j.jcis.2014.10.034

515 Hu Z, Patten T, Pelton R, Cranston ED (2015b) Synergistic Stabilization of Emulsions and Emulsion
516 Gels with Water-Soluble Polymers and Cellulose Nanocrystals. ACS Sustain Chem Eng
517 3:1023–1031. doi: 10.1021/acssuschemeng.5b00194

518 Jiang Y, Liu X, Chen Y, et al (2014) Pickering emulsion stabilized by lipase-containing periodic
519 mesoporous organosilica particles: A robust biocatalyst system for biodiesel production.
520 Bioresour Technol 153:278–283. doi: 10.1016/j.biortech.2013.12.001

521 Kalashnikova I, Bizot H, Bertoncini P, et al (2013) Cellulosic nanorods of various aspect ratios for oil
522 in water Pickering emulsions. Soft Matter 9:952–959. doi: 10.1039/C2SM26472B

523 Kalashnikova I, Bizot H, Cathala B, Capron I (2011) New Pickering emulsions stabilized by bacterial
524 cellulose nanocrystals. Langmuir ACS J Surf Colloids 27:7471–7479. doi: 10.1021/la200971f

525 Kari Koskenhely (2008) Refining of chemical pulp fibers. In: Papermaking Part 1, Stock preparation
526 and wet end. Finnish paper engineers' association,

527 Katz S, Beatson RP, Scallan AM (1984) The determination of strong and weak acidic groups in
528 sulfite pulps. Sven. Papperstidning 795–816.

529 Kester DR, Duedall IW, Connors DN, Pytkowicz RM (1967) Preparation of artificial seawater. Limnol
530 Oceanogr 12:176–179. doi: 10.4319/lo.1967.12.1.0176

531 Nyankson E, DeCuir MJ, Gupta RB (2015) Soybean Lecithin as a Dispersant for Crude Oil Spills. ACS
532 Sustain Chem Eng 3:920–931. doi: 10.1021/acssuschemeng.5b00027

533 Ojala J, Sirviö JA, Liimatainen H (2016) Nanoparticle emulsifiers based on bifunctionalized cellulose
534 nanocrystals as marine diesel oil–water emulsion stabilizers. Chem Eng J 288:312–320. doi:
535 10.1016/j.cej.2015.10.113

536 Orelma H, Tanaka A, Rautkoski H, et al (2017) Mechanically ground softwood fines as a raw
537 material for cellulosic applications. Cellulose 24:3869–3882. doi: 10.1007/s10570-017-
538 1403-x

539 Pi G, Li Y, Bao M, et al (2016) Novel and Environmentally Friendly Oil Spill Dispersant Based on the
540 Synergy of Biopolymer Xanthan Gum and Silica Nanoparticles. ACS Sustain Chem Eng
541 4:3095–3102. doi: 10.1021/acssuschemeng.6b00063

542 Prince RC (2015) Oil Spill Dispersants: Boon or Bane? Environ Sci Technol 49:6376–6384. doi:
543 10.1021/acs.est.5b00961

544 Rattaz A, Mishra SP, Chabot B, Daneault C (2011) Cellulose nanofibres by sonocatalysed-TEMPO-
545 oxidation. Cellulose 18:585–593. doi: 10.1007/s10570-011-9529-8

546 Saha A, Nikova A, Venkataraman P, et al (2013) Oil Emulsification Using Surface-Tunable Carbon
547 Black Particles. ACS Appl Mater Interfaces 5:3094–3100. doi: 10.1021/am3032844

548 Silva MC, Lopes OR, Colodette JL, et al (2008) Characterization of three non-product materials
549 from a bleached eucalyptus kraft pulp mill, in view of valorising them as a source of
550 cellulose fibres. Ind Crops Prod 27:288–295. doi: 10.1016/j.indcrop.2007.11.005

551 Sirvio J, Hyvakko U, Liimatainen H, et al (2011) Periodate oxidation of cellulose at elevated
552 temperatures using metal salts as cellulose activators. Carbohydr Polym 83:1293–1297.
553 doi: 10.1016/j.carbpol.2010.09.036

554 Tadros TF (ed) (2013) Emulsion formation and stability. Wiley-VCH, Weinheim

555 Wang W, Zheng Y, Lee K (2013) Chemical dispersion of oil with mineral fines in a low temperature
556 environment. Mar Pollut Bull 72:205–212. doi: 10.1016/j.marpolbul.2013.03.042

557 Xhanari K, Syverud K, Stenius P (2011) Emulsions Stabilized by Microfibrillated Cellulose: The Effect
558 of Hydrophobization, Concentration and O/W Ratio. J Dispers Sci Technol 32:447–452. doi:
559 10.1080/01932691003658942

560 Yu G, Dong J, Foster LM, et al (2014) Breakup of Oil Jets into Droplets in Seawater with
561 Environmentally Benign Nanoparticle and Surfactant Dispersants. Ind Eng Chem Res
562 141223085223001. doi: 10.1021/ie503658h

563 Zeinstra-Helfrich M, Koops W, Murk AJ (2015) The NET effect of dispersants — a critical review of
564 testing and modelling of surface oil dispersion. Mar Pollut Bull 100:102–111. doi:
565 10.1016/j.marpolbul.2015.09.022

566 Zhang Y, Chen D, Ennis AC, et al (2013) Chemical dispersant potentiates crude oil impacts on
567 growth, reproduction, and gene expression in Caenorhabditis elegans. Arch Toxicol
568 87:371–382. doi: 10.1007/s00204-012-0936-x

569